Nanoscale

RSC Publishing

FEATURE ARTICLE

View Article Online
View Journal | View Issue

Intelligent, self-powered, drug delivery systems

Cite this: *Nanoscale*, 2013, **5**, 1273

Debabrata Patra, Samudra Sengupta, Wentao Duan, Hua Zhang, Ryan Pavlick and Ayusman Sen*

Received 4th September 2012
Accepted 11th October 2012

DOI: 10.1039/c2nr32600k

www.rsc.org/nanoscale

Self-propelled nano/micromotors and pumps are considered to be next generation drug delivery systems since the carriers can either propel themselves ("motor"-based drug delivery) or be delivered ("pump"-based drug delivery) to the target in response to specific biomarkers. Recently, there has been significant advancement towards developing nano/microtransporters into proof-of-concept tools for biomedical applications. This review encompasses the progress made to date on the design of synthetic nano/micromotors and pumps with respect to transportation and delivery of cargo at specific locations. Looking ahead, it is possible to imagine a day when intelligent machines navigate through the human body and perform challenging tasks.

1 Introduction

The evolution of nanotechnology has allowed us to develop synthetic nanodevices for various tasks and diverse applications. One important area is nano-medicine where therapeutic diagnosis and site-specific drug delivery are of key importance. The current research on drug delivery focuses on specific problems like targeted delivery,[1] solubility issues of drugs,[2] protecting drugs from biochemical degradation and controlling the therapeutic payload.[3,4] In the past few decades, nanoscale vectors *e.g.* nanoparticles,[5] emulsions,[6] micelles[7] and liposomes[8] have been constructed for drug delivery. However, these systems rely on the circulatory system and the carriers are only "passively" conveyed towards the targets. Accordingly, it would be interesting to develop drug delivery systems that can manipulate the local flow and the carriers can either propel themselves ("motor"-based drug delivery systems) or be delivered ("pump"-based drug delivery systems) to the target in response to specific biomarkers.

Such motors and pumps are well-known in living systems.[9–11] Biological motors are found as proteins and nucleic acids and involve mechanoenzymes that transduce chemical energy into mechanical energy. Nucleic acid motors include RNA polymerases (transcribe RNA from DNA) as well as DNA polymerases (produce double-stranded DNA from single stranded DNA) and protein motors include myosins (responsible for muscle contractions), kinesins (carry cargo along microfilaments

Department of Chemistry, Pennsylvania State University, University Park, PA 16802, USA. E-mail: asen@psu.edu

Debabrata Patra obtained his M.Sc. in Chemistry from the Indian Institute of Technology, Bombay in 2005 and received his Ph.D. degree in 2010 from the Department of Chemistry at the University of Massachusetts, Amherst, under the tutelage of Prof. Vincent M. Rotello. Currently, he is working as a postdoctoral associate under the direction of Prof. Ayusman Sen at the Pennsylvania State University, University Park. His current research is focused on designing supramolecular micropumps based on molecular recognitions. He is also investigating enzyme powered devices such as enzyme powered micropumps and micromotors.

Samudra Sengupta was born in Kolkata, India. He received his M.Sc. in Chemistry from St Stephen's College, Delhi University, Delhi in 2007. He is currently working towards his Ph.D. under the guidance of Prof. Ayusman Sen at the Pennsylvania State University. His research interests include single-molecule studies and designing new enzyme-based devices. He recently received the Materials Research Institute Fellowship at the Pennsylvania State University. In his free time he enjoys playing soccer.

within a cell) and dyneins, which are responsible for ciliary and flagellar motility.[12] As for the biological pump systems, one of the well-known examples is efflux pumps which offer resistance to therapeutic drugs for diverse biological systems ranging from relatively simple bacterial cells to complex human cancer cells. These biological pumps decrease the intracellular concentration of the drug to subtoxic levels.[13–16]

Inspired by the remarkable performance of biological motors and pumps, research effort has shifted towards incorporating motor proteins into synthetic systems to create function-specific hybrid bio-synthetic nanomotors.[17,18] In one instance, cargo was nonspecifically (electrostatically/hydrophobically) attached onto kinesin and showed unidirectional transport of materials such as gold, polystyrene, and glass.[19,20] In another example, a synthetic motor in conjunction with biomolecular motors such as F_1-ATPase (F_1-adenosine triphosphate synthase) was able to produce self-propelled motion in the presence of ATP, adenosine triphosphate (Fig. 1a).[21] In addition, several other groups reported attempts to integrate living organisms into micromechanical devices to understand their behavior for microtransport systems (Fig. 1b).[22] For example, Uyeda *et al.* immobilized gliding *Mycoplasma mobile* bacteria onto a microrotary motor which can generate motion in the presence of a specific fuel like glucose (Fig. 1b).[23] Similarly, Berg *et al.* demonstrated that flagellated bacteria when adsorbed at a solid–liquid interface can create motion in the surrounding fluid with potential applications in fluid pumping.[24]

Besides the considerable promise of biomotors/hybrid biomotors, in the past decade an interdisciplinary research area has emerged to address the challenges of self-propulsion at the nano/micro length scale in synthetic systems. The motion of the artificial nano/microbots does not rely on the motor proteins or the living organism; it solely depends on the catalytic reaction at the bot–fluid interface. These nano/microscale devices have a wealth of potential applications which have been discussed in

Wentao Duan received his B.S. degree in Chemistry at Yuanpei College, Peking University (P.R. China). He then joined the nanomotor research group at the Pennsylvania State University to pursue his Ph.D. degree under the supervision of Prof. Sen. His research interest includes designing nanomotors that exhibit collective behavior and exploring and modeling the diffusional property of nanomotors.

Ryan Pavlick was born and grew up in East Brunswick, New Jersey. He started his science career at the College of New Jersey obtaining his Bachelors of Science in chemistry. While there he participated in research studying bioactive organometallic complexes under Dr Georgia Arvanitis. He also spent time at Clemson University doing an REU studying solid-state ceramics in Shiou-Jyh Hwu's group. He is currently working at the Pennsylvania State University in the chemistry department in Dr Ayusman Sen's group. His work is on using organometallics to develop self-motile and directed repair systems.

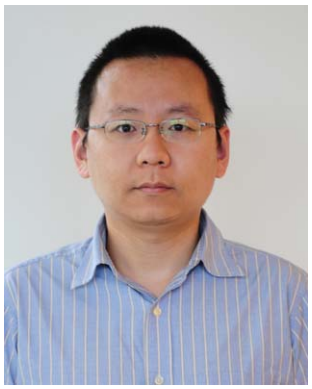

Hua Zhang was born in Zhengzhou, China. He received his Bachelor degree of Chemistry from Wuhan University. Later, he graduated from Wuhan University with a Master degree in polymer chemistry and physics. He joined Dr Sen's group in 2007. His research interests cover antibacterial polymers/materials and polymer-based micromotors and micropumps. His hobbies include photography and scale modeling.

Ayusman Sen was born in Calcutta, India and holds a Ph.D. from the University of Chicago where he was first introduced to catalysis. Following a year of postdoctoral work at the California Institute of Technology, he joined the Chemistry Department of the Pennsylvania State University where he is currently a Distinguished Professor. He is a Fellow of the American Association for the Advancement of Science. His research interests encompass catalysis, organometallic and polymer chemistry, and nanotechnology. He is the author of approximately 300 scientific publications and holds 24 patents. Sen's pastime centers on enological and gastronomical explorations.

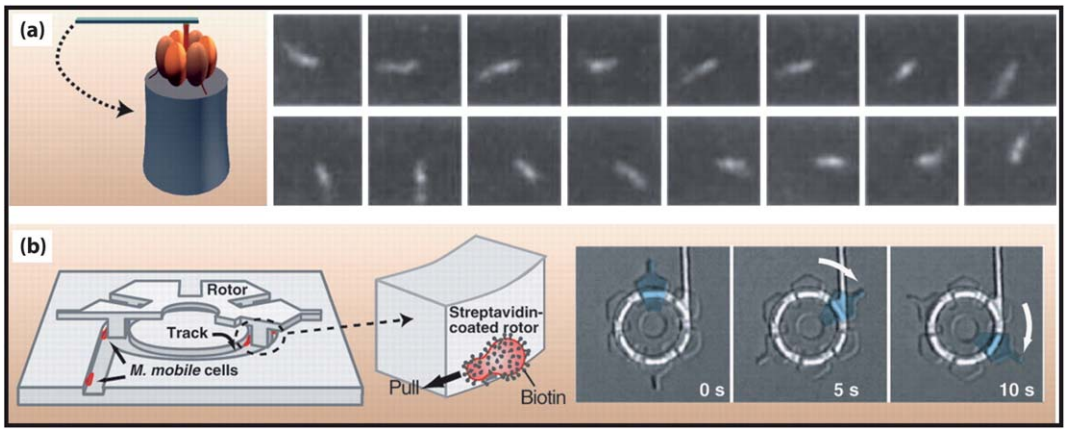

Fig. 1 (a) An F_1-ATPase-powered nanopropeller and the rotary motion of the F_1-ATPase motor by using a fluorescent actin filament connected to the stalk. (b) A bacteria powered microrotor (20 mm diameter) (from ref. 22).

several review papers.[25–31] In this perspective, we discuss artificial self-propelled systems which have been used as vehicles for cargo transportation, cargo delivery and micropumping, and their potential applications in drug delivery.

2 Transport at the nanoscale: important physical parameters

As one approaches the nano/microscale, the physics begins to alter from that in the normal macroscopic world. Two important concepts to realize at small scales are viscous drag and Brownian randomization. A way to examine if the former is important to a system is to look at the Reynolds number:

$$\mathrm{Re} = \frac{\rho V l}{\eta}$$

where Re is the Reynolds number, ρ is the density of the fluid, V is the velocity of the particle of interest, l is the length scale of the system, and η is the viscosity of the system.[32] This number relates to the ratio of inertial forces to viscous forces. So the higher the number, the more the inertial forces dominate in the system; conversely, the lower the number, the more effective are the viscous forces. To put this in perspective, the approximate Reynolds numbers for three species swimming in water are: human, 10^4; fish, 10^2; and bacterium, 10^{-4}. Self-powered delivery systems designed for living organisms operate in the low Reynolds number regime; hence viscous forces dominate. This means that if a motile force is applied to the system it will nearly instantaneously be counteracted by the viscous drag of the fluid. The system thus reaches its terminal velocity very quickly and contains insignificant momentum.

Another effect that is prominent in systems with low Reynolds number is Brownian motion. Brownian motion is the thermally driven collisions of solvent molecules with colloidal particles that cause an observed random motion of the particles.[33] This is a problem when designing directed systems because these collisions work to alter the trajectory of the motor particle. Random Brownian diffusion can be defined by the Stokes–Einstein relationship as follows:

$$D = \frac{kT}{6\pi\eta r}$$

where the diffusion coefficient D is related to the thermal energy in the system, k is the Boltzmann constant, and T corresponds to the absolute temperature. The denominator $6\pi\eta r$ corresponds to Stokes' relationship relating viscous drag to the particle size where r is the radius of the particles and η is the viscosity of the liquid. As spherical particles move through water they encounter a viscous drag that limits diffusive steps. An important thing to note from the equations is that as the particle size decreases thermal collisions in the system lead to more random motion and reorientation.

3 Artificial nano- and micro-devices as delivery vehicles

The first wholly synthetic autonomous nanomotor was synthesized by Paxton *et al.*[34] in 2004 followed closely by Fournier-Bidoz *et al.*[35] Motivated by these efforts, several kinds of artificial autonomous microengines powered by catalytic reactions have been realized thus far. In many cases, bubble propulsion turns out to be the governing force and hydrogen peroxide (H_2O_2) continues to dominate as the fuel. In this section we will summarize the efforts to design self-powered artificial nano/microdevices which are made of inorganic nano/microparticles and aimed for cargo towing and delivery applications.

3.1 Nano/microrod transporter

3.1.1 Basic design and principle. The fundamental design of self-propelled nanomotors was first demonstrated by Sen *et al.* using an Au–Pt bimetallic nanorod ($l = 2$ μm; $w = 370$ nm). The nanorods move autonomously in hydrogen peroxide solution at a speed of 5–10 μm s^{-1}, the platinum end facing forward. The movement of the nanorod was attributed to the asymmetric electrocatalytic decomposition of H_2O_2. Oxidation of H_2O_2 to O_2 occurs at the Pt anode and reduction to H_2O occurs at the Au cathode. This creates a proton gradient along the axis of the rod from the Pt to Au. As a result, the negatively charged microrod

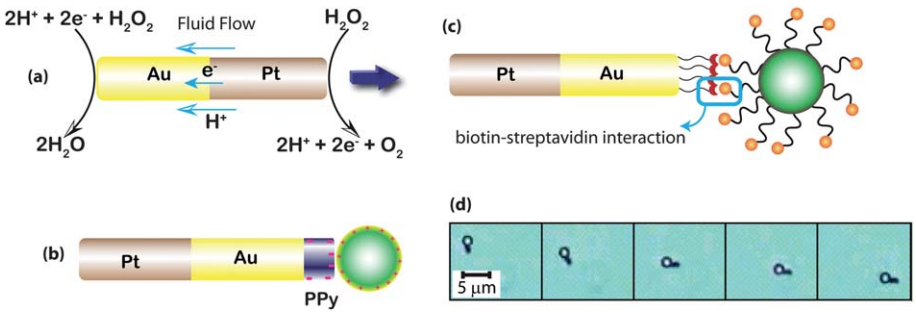

Fig. 2 (a) Schematic of motion of a Pt–Au nanorod driven by the catalytic decomposition of hydrogen peroxide. Attachment of cargo with a nanomotor *via* (b) biotin–avidin interaction and (c) electrostatic assembly. (d) Cargo pulling by the Pt–Au–PPy motor; the trajectory over 4 s (from ref. 37).

responds by moving forward towards the proton rich region *via* a self-electrophoretic mechanism (Fig. 2a).[36]

3.1.2 Cargo transportation and delivery. Later, using this principle the same group demonstrated the cargo towing ability of bimetallic rods and elucidated systematic trends in motor speed as a function of cargo radius. In their work they synthesized Pt–Au, Pt–Au–PPy and Pt–Ni–Au–Ni–Au–PPy rods using a traditional electrochemical deposition technique; Ni was introduced for steering the rod magnetically to minimize enhanced rotational diffusion of the rod.[37] The prototype cargo can be attached to the tip of the motor using two methods: (i) electrostatic interaction: positively charged polystyrene amidine cargo was attached to a negatively charged PPy (polypyrrole) segment at the end of the rod; (ii) biotin–streptavidin interaction: this method relies on a more specific biotin–avidin interaction, where the Au end of the Pt–Au rod was functionalized with biotin and polystyrene was coated with streptavidin (Fig. 2b and c). Cargo of various radii ranging from 0.38–1.05 μm show different translational motions in the presence of hydrogen peroxide. Fig. 2d shows self-propulsion of a Pt–Au–PPy motor carrying a prototype cargo of radius 1.05 μm.

A key attribute of a delivery device is its ability to release cargo at will for real life applications. Efforts have been made to demonstrate on-demand cargo release by synthetic nanomotors. Both exogenous (light, magnetic field) and endogenous (chemical stimuli) activation strategies have been exploited for triggering the cargo release. Using Pt–Au–Ag–Au–PPy catalytic nanomotors, the Sen group has shown a prototype cargo release by selective dissolution of an Ag segment in the presence of chloride ions, peroxide and UV light. A cargo drop-off was observed within 10–20 s of UV-light exposure.[38] In another method of cargo drop-off, a photocleavable linker was used to attach the motor to the cargo (Fig. 3a). Irradiation with UV light cleaves the bond leading to cargo drop-off. The speed of the motor–cargo doublet was 2.3 μm s^{-1} and after unloading the cargo, the speed of the motor increased up to 4.8 μm s^{-1} due to reduction of the drag force after cargo release (Fig. 3b). In a study involving magnetically controlled transport, catalytic nanomotors [Ni/(Au/Ag)/Ni/Pt] were shown to pick-up and transport drug-loaded, iron oxide encapsulated-polymeric microparticles and liposomes in microfluidic channels, and release them at desired locations (Fig. 3c).[39] Wang's group also reported the transport of cargo bound to Au–Ni–Au–Pt-CNT nanorods (Fig. 3d) and their controlled release in a microfluidic channel.[40] In both the systems, the nanorods transport their respective cargos at high speeds.

3.1.3 Motion-based sensing. Au–Pt nanorods have been used for the detection of trace amounts of silver in solutions

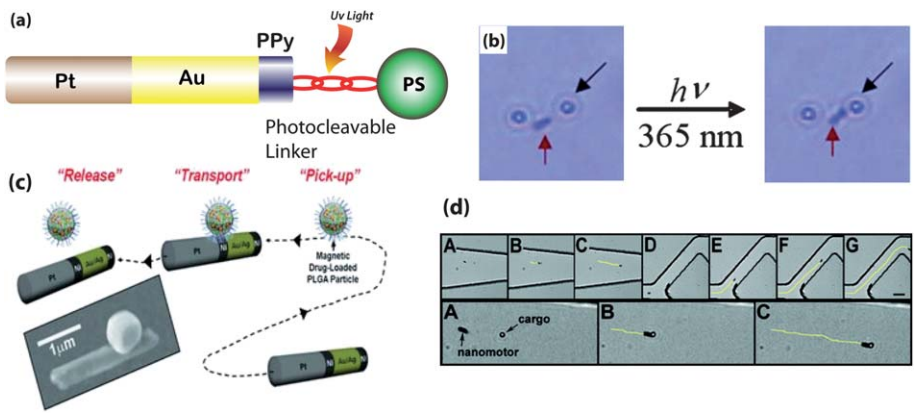

Fig. 3 (a) Schematic image of the motor design for photo crosslinker assisted cargo drop-off. (b) Optical microscopy images of UV triggered drop of cargo (from ref. 38). (c) Scheme depicting the dynamic pick-up, transport, and release of drug-loaded PLGA particles using a nanoshuttle (from ref. 39). (d) Optical microscopy images of the dynamic loading of an Au–Pt-CNT nanomotor with a magnetic microparticle and cargo transport in PDMS (from ref. 40).

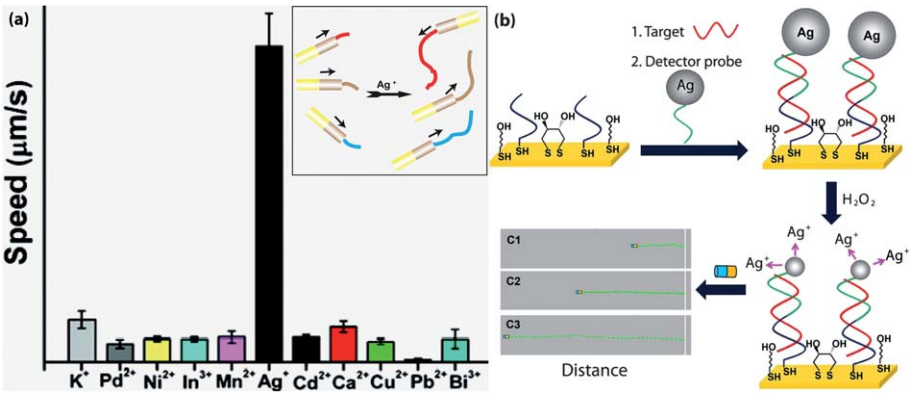

Fig. 4 (a) Motion of Au–Pt catalytic nanomotors in a 5% H_2O_2 solution containing 11 common cations (from ref. 41). (b) Step-wise motion-based nucleic acid detection: hybridization of target, capture of the Ag nanoparticle-tagged detector probe, dissolution of silver nanoparticle tags in the peroxide fuel; visual detection of the motion of the catalytic nanowire motors (from ref. 42).

with significant selectivity.[41] The speed of the nanomotors increases in the presence of silver ions in a concentration-dependent manner (Fig. 4a). This technique offers high sensitivity as it can detect nanomolar levels of silver ions. As an extension of their work involving the dependence of motor speed on silver ion concentration, Wang and co-workers have devised a sensing tool for biodetection of nucleic acids by monitoring the speed of the Au–Pt micromotors.[42] The motion based assay involves duplex formation of the nucleic acid target with a thiolated DNA capture probe and a silver nanoparticle-tagged detector probe (Fig. 4b). The speeds of the Au–Pt nanomotors were monitored in a solution of silver ions generated by the dissolution of captured nanoparticles in hydrogen peroxide. The higher the concentration of the target probe, the greater the number of silver nanoparticles captured, and therefore, the higher the speed of the nanomotor upon silver dissolution. This bioanalytical technique has an extremely high sensitivity, down to the attomole level of the target nucleic acid. By further improving the signal to background properties ultrasensitive DNA biosensors have been designed, with detection limits in the zeptomolar range.[43]

3.2 Janus sphere transporter

3.2.1 Basic design and principle. Spherical colloidal particles are found to be attractive candidates for cargo delivery applications as they are cost effective, easy to synthesize and have great potential in immunoassay as well as cancer therapy. In order to achieve the directed motion, we need to break the symmetry of a spherical particle *i.e.* a Janus type asymmetry is required. Autonomous propulsion of Janus particles was reported earlier but their ability to transport cargo was first shown by Schmidt *et al.*[44] In this work, Baraban *et al.* fabricated a catalytic Janus motor by bottom-up self-assembly of silica colloidal particles followed by the deposition of a magnetic layer system (Co and Pt multilayer stack; Fig. 5a). The propulsion of Janus spheres was observed in the presence of 10% H_2O_2 solution with a speed of 8 μm s^{-1} and their direction was precisely controlled by an external magnetic field of 10 Oe.

3.2.2 Cargo transportation and delivery. The manipulation of cargo was later realized by applying magnetic field. In their experiment, they mixed the superparamagnetic cargo (r = 5 μm) with a suspension of Janus motor particles. The external magnetic field reorients the magnetic cap of the motor as well as induces a net magnetic moment to the superparamagnetic cargo. As a result there is a magnetic dipole–dipole interaction between the magnetic moment of the cargo and the motor. This induced moment helped to attach the cargo

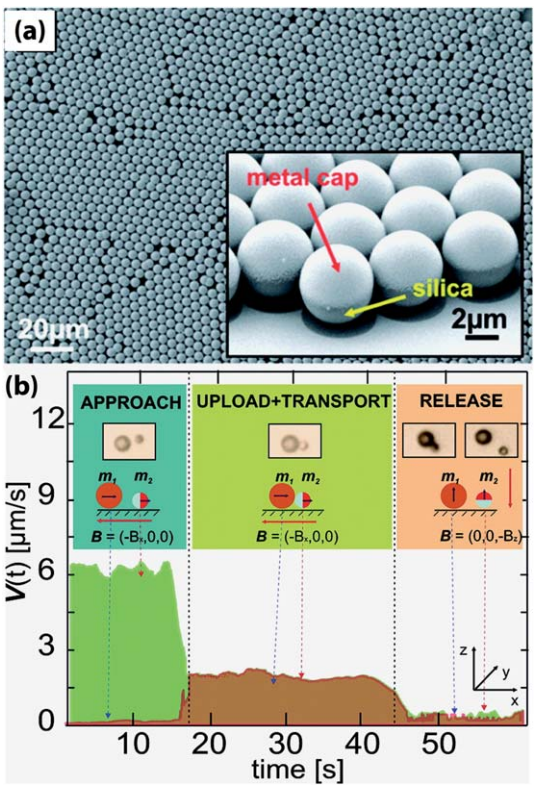

Fig. 5 (a) Scanning electron microscopy image of Janus particles with a metal film on top. (b) Controlled motion of the Janus particles can be achieved by orienting the external magnetic field (from ref. 44).

to the motor particles. However, this interaction can be switched to repulsive by changing the orientation of the magnetic field which resulted in releasing the cargo from the vector (Fig. 5b).

3.3 Microtube transporter

3.3.1 Basic design and principle. Recently, rolled-up nanotubes, a new class of nanostructured materials, have attracted attention due to easy motion control, high speeds, integration of various functions and straight trajectories compared to traditional self-propelled micromotors.[45] These microjet-like structures can be propelled in biological and high ionic-strength fluids.[46,47] The catalytic version of the rolled-up nanotube was first fabricated by Schmidt and coworkers; the microtube consists of (i) a catalyst layer, usually Pt, (ii) a magnetic layer, Fe for magnetic manipulation, and (iii) a Ti/Au layer for good adhesion between layers.[48] In general, a pre-stressed, multimetallic thin film deposited onto a sacrificial photoresist layer is released from the substrate surface by etching away the photoresist. The layer then spontaneously rolled up and formed a microtube [l = 100 μm; d = 5.5 μm; Fig. 6a and b].

Another type of tubular microengine was synthesized by Wang *et al.* using an electrochemical growth of bilayer polyaniline/platinum microtubes within the conically shaped pores of a polycarbonate template membrane (Fig. 6c–e). These microjets (8 μm in length) are self-propelled at a high speed (>350 body length per s) and can operate at a very low fuel concentration (0.2%).[49] When the microtubes are immersed in hydrogen peroxide solution, oxygen microbubbles are generated inside the cavity of the tubes and are released from one opening. This bubble propulsion force drives the tubes directionally with high speeds.

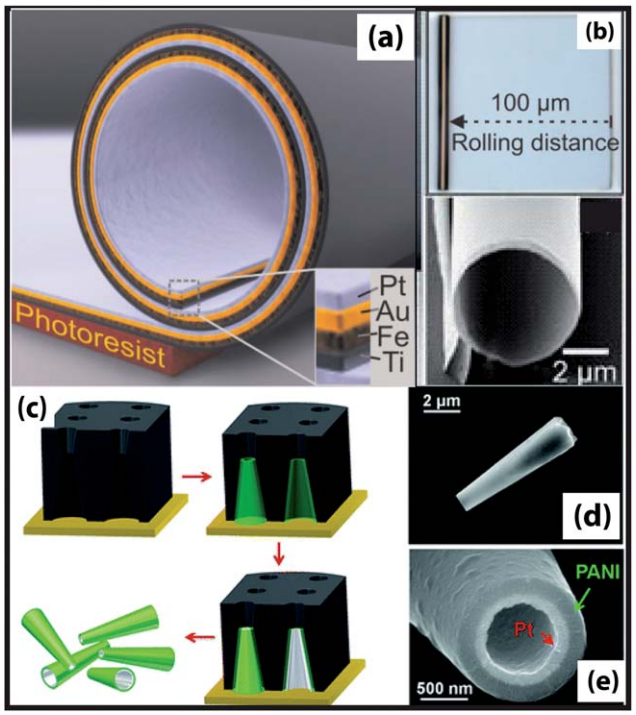

Fig. 6 (a) Schematic diagram of a rolled-up microtube consisting of Pt/Au/Fe/Ti multilayers on a photoresist sacrificial layer. (b) Optical microscopy and SEM images of a rolled-up Pt/Au/Fe/Ti microtube (from ref. 48). (c) Schematic of preparation of bilayer PANI/Pt microtubes using cyclopore polycarbonate membranes. SEM images of the microtube engines: (d) side view and (e) cross view of a bilayer PANI/Pt microtube (from ref. 49).

3.3.2 Cargo transportation and delivery. The loading of multiple cargos on a single nanomotor, preloading functionalization, *i.e.* cargo specific functionalizations, and reusability are current challenges in the area of motor-based delivery systems. In this regard, the rolled-up microtubes motors have several advantages. They exhibit high propulsion power which allows simultaneous transport of multiple microparticles, as well as metallic nanoplates. The loading of particles was also achieved by the pumping of fluid into the microtubes *via* a catalytic reaction. The suction of fluid into microtubes induces an inward fluid motion that streamlines near the entrance of the tubes; as a result the nearby particles are absorbed at the entrance of the tubes. The direction of the motion of the tubes was controlled by altering the magnetic field, and the cargo was released by a rapid turn of the magnet.[50] The first example of a real biological cargo was given by Sanchez *et al.* using Pt/Ti/Fe microtubes. They reported the loading, carrying and release of CAD (cathecolaminergic cell line from the central nervous system; 10–15 μm) cells using these micromachine transporters (Fig. 7a).[51] The microbots were self-propelled in 4% H_2O_2 solution with an initial speed of 130 μm s^{-1} (before loading) and reduced to 60 μm s^{-1} after the loading of CAD cells as the drag force increases (Fig. 7b). In another work, Schmidt *et al.* discovered that asymmetry in the shape of the rolled-up tube can alter their trajectories in liquid and offered new functionalities (Fig. 7c). They used molecular beam epitaxy (MBE) to fabricate InGaAs/GaAs/Cr(Pt) tubes and shape asymmetry was done by scratching the tube in different directions. The release of bubbles from these rolled-up structures was asymmetric in nature (Fig. 7d); as a result microtubes moved in helical trajectories. These nanotools have been utilized as a shuttle for yeast and HeLa cells. The drilling behavior of nanotools into biomaterials was also explored.[52]

3.3.3 Motion-based isolation. The Wang group has made significant contributions to motion-based isolation of biomolecules in complex biological matrices. The motion based target hybridization and isolation were demonstrated using DNA functionalized microtubes (Fig. 8a and b). The microrockets propelled within the biological sample (containing the fuel) and interact with the target nucleic acid (complementary DNA or bacterial rRNA) tagged with fluorescent nanoparticles. More interestingly, the functionalized microrockets were able to transport the captured target through a microchannel toward a "clean" downstream zone, thus providing dynamic single-step extraction for subsequent analysis.[53] A similar strategy was applied for the selective capture of pathogenic bacteria which opens up an attractive avenue for motion based theranostics. In this case, lectin functionalized microtubes recognized the specific terminal carbohydrates of *E. coli* surface polysaccharides during their propulsion in solution. The captured

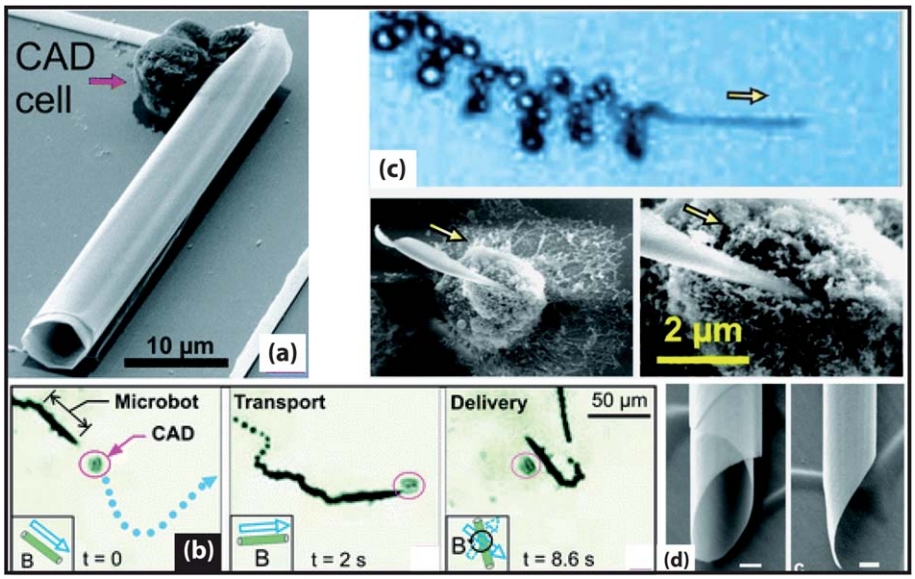

Fig. 7 (a) SEM images of Ti/Fe/Pt rolled-up microtubes with CAD cells, (b) controlled manipulation of CAD cells by using catalytic microbots using magnetic field (from ref. 51), (c) corkscrew-like trajectory of microbots and SEM images of an active nanotool drilling into a cross-linked biomaterial and (d) SEM images of rolled-up nanotubes with cylindrical and asymmetric geometries (from ref. 52).

bacteria were selectively released from the micromotor in a low pH glycine solution, which breaks the lectin–bacteria conjugate (Fig. 8c).[54] In a similar approach, tubular nanorods were used for selective isolation of thrombin protein from complex biological samples, and their transport and ATP-assisted release.[55] The microrockets were functionalized with aptamers, which have high selectivity and affinity for thrombin. The high selectivity and binding affinity aid in capturing the target protein and transporting it to a desired location. Introducing ATP into the solution, which displaces the thrombin from the aptamer, triggered the controlled release of the protein. These microrockets can selectively capture and transport proteins from complex biological fluid samples like serum and plasma. The most fascinating work in this area is the custom designing of a microengine for cancer cell pickup and separation from a mixture of cell lines. Antibody functionalized microengines showed preferential binding for antigenic surface proteins expressed on cancer cells (Fig. 8d). This technique holds great promise for extracting cancer targeting cells from biological fluids and hence for the early diagnosis of cancer.[56]

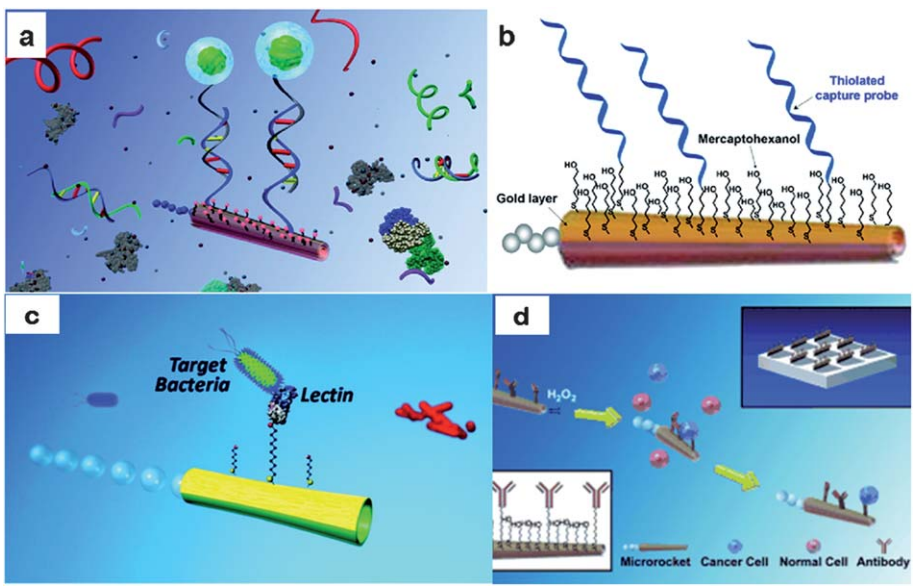

Fig. 8 (a) Schematic of the motion-based target hybridization and isolation process from raw biological samples. (b) Surface functionalization of microrockets with the binary SAM (from ref. 53). (c) Lectin ConA-modified microengine for selective pick-up, transport and release of bacteria (from ref. 54) (d) Anti-CEA mAb-modified microrockets recognize the CEA surface antigens on the target cancer cells, allowing their selective pickup and transport (from ref. 56).

4 Micropumps design and their applications

There is an increasing interest in making micropumps which are designed to handle a small amount of fluid at a well-described and preferably programmable rate.[57] The application areas of micro-pumps include microanalytical instrumentation, genetic engineering, portable sampling systems and drug delivery.[58–63] A number of micropumps with different actuating principles and fabricated by different technologies have been reported in the literature.[64,65] In this section we discuss the design and applications of self-powered micropumps.

4.1 Electrochemical micropumps

In previous sections, we discussed the design and fabrication of various micromotor systems. By Galilean invariance, immobilized micromotors should create a flow in surrounding fluids, with similar scaling in device size and fluid velocity. Following their previous work on bimetallic Au–Pt nanomotors, Sen *et al.* developed a micropump system using the same principle. This micropump is fabricated by the deposition of a silver pattern on a gold-coated substrate (Fig. 9).[66] In the presence of hydrogen peroxide solution, the Ag–Au bimetallic structure catalytically decomposes hydrogen peroxide *via* the following electrochemical process:

$$\text{Overall: } H_2O_2 \rightarrow 2H_2O + O_2;\ E = 1.1\ \text{V}$$

$$\text{Anode (Au): } H_2O_2 \rightarrow O_2 + 2H^+ + 2e^-$$

$$\text{Cathode (Ag): } H_2O_2 + 2H^+ + 2e^- \rightarrow 2H_2O_2$$

The resulting electric field generates convective flow inside a closed chamber of liquid. The fluid flow, as well as the motion of tracers, depends on two parameters, (i) electroosmotic flow (v_{eo}): proton gradient causes the flow and (ii) electrophoretic movement (U): depends on the zeta potential of the tracers. In the actual experiment, the electroosmotic component was found to dominate at longer distances leading to convective rolls in a closed system (Fig. 9). Besides Au–Ag micropumps, Au–Pd bimetallic pumps were also discovered using different fuel combinations such as hydrazine and *asym-N,N*-dimethylhydrazine.[67] Inspired by bimetallic micropumps, Jun and Hess invented a compartmentalized micropump using electrochemical decomposition of hydrogen peroxide.[68] In their work, they used a polycarbonate membrane with Au deposited on one side and Pt deposited on the other side (Fig. 10a). The platinum electrode and the gold electrode are electrically connected by an external switch. Hydrogen peroxide decomposition on the platinum electrode produces protons and electrons. While electrons move through the external circuit, the hydrated protons migrate towards the gold electrode through the micropores. As a result, each pore on the membrane is able to generate a tiny electroosmotic flow across the membrane. The concept of self-pumping can lead to the creation of artificial biological membranes which can harvest chemical energy from the surrounding fluid and use it for mass transportation across the membrane.

4.2 Photocatalytic micropumps

The design of a micropump with stimuli responsive properties is of great interest for applications ranging from drug delivery to microfluidics. In particular, light-induced pumping is interesting as it offers the possibility of remote control with an external physical stimulus. The first light triggered prototype micropump was shown by Sen's group using TiO_2 particles.[69] Titanium dioxide (TiO_2) possesses high photocatalytic property which can be utilized to power the autonomous motion of microscale objects. Before this micropump is turned on, silicon tracer particles gather around TiO_2 particles. Under UV exposure TiO_2 produced multiple ionic species. Due to the difference in diffusivity between the ions a net electric field was then set up around the TiO_2 micropumps, which pushed charged tracer

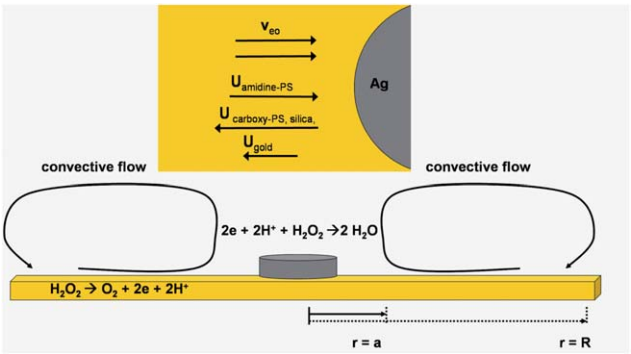

Fig. 9 Schematic of Au–Ag micropump operated by the oxidation of peroxide. U represents the diffusiophoretic velocity of specific tracer particles and v_{eo} the electroosmotic fluid flow (from ref. 66).

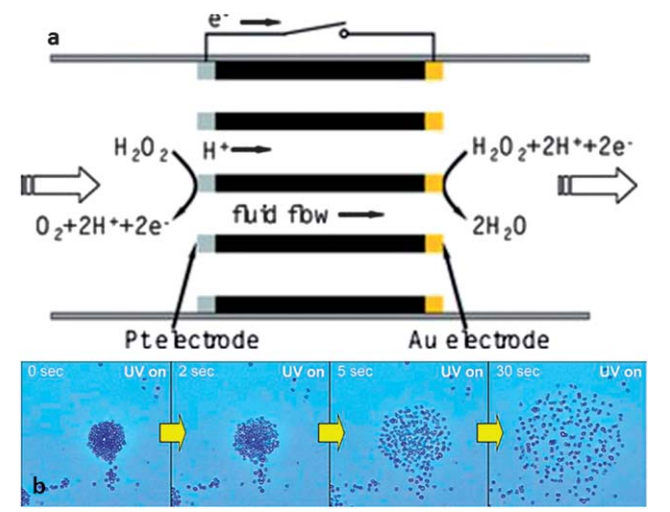

Fig. 10 (a) The self-pumping membrane made of gold and platinum electrodes and deposited on the opposing surfaces of a track-etched polycarbonate membrane (from ref. 68). (b) The SiO_2–TiO_2 Janus particles in deionized water aggregated in the absence of UV and repelled each other when UV is switched on. The process is reversible (from ref. 69).

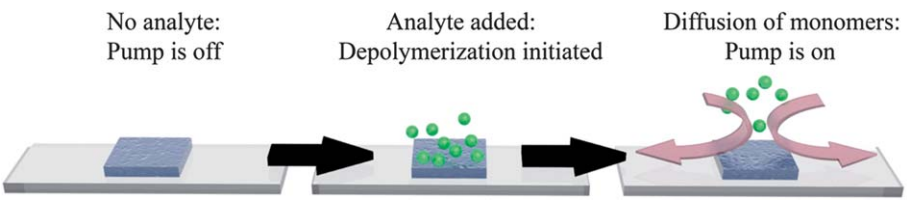

Fig. 11 Schematic and mechanism of a depolymerization micropump. The blue piece represents the polymer film, green spheres represent monomers or small molecules after depolymerization, and pink arrows show overall fluid flow.

particles to move in a directional fashion depending on their own surface charge (ζ potential). This electrolyte diffusiophoresis flow can be shut down in high ionic strength solutions. The resultant flow decides the motion of the tracers. The spatial arrangement of the tracers around TiO_2 particles was termed as "microfireworks" and it was turned on/off reversibly by light (Fig. 10b).

4.3 Analyte induced micropumps

Very recently, Sen and Phillips *et al.* reported a whole new concept of a micropump which can sense analytes in solution and, in response, trigger fluid flow. The working principle of the pump is based on analyte-initiated depolymerization.[70] The team used two different polymers: (i) *tert*-butyldimethylsilyl (TBS) end-capped poly (phthalaldehyde) (TBS-PPHA), which reacts to fluoride and (ii) poly(ethyl cyanoacrylate) (PECA), which responds to high pH. This particular micropump system has unique features such as (i) it can be turned on by specific chemical or biological signals and (ii) it does not require an external power source. Further, the depolymerization of a single polymer chain is triggered by one analyte molecule leading to a large number of monomer products; this results in considerable signal amplification and accompanies high sensitivity to the analyte. The micropump was fabricated by simply spin casting a thin film of TBS-PPHA or PECA on a glass slide. In the presence of an anion initiator such as fluoride or hydroxide, the polymer depolymerizes and creates a concentration gradient that pumps fluids and insoluble particles away from the bulk polymer by a diffusiophoretic mechanism (Fig. 11). These pumps are capable of moving fluids and micrometer-scale particles autonomously over long distances with velocities that can be tuned by the concentration of the specific analytes. The group has also shown the sensing ability of the micropump using a combination of a detection agent and a biomarker. In the presence of the biomarker (*e.g.*, enzyme), the detection agent produces analytes which turn on the pump. In principle, the concept can be employed for drug delivery "on demand," such as an insulin-loaded micropump implanted inside the body which is turned on by high glucose level in the bloodstream.

5 Conclusion and future scope

We have highlighted the potential opportunities that the self-powered nano/microbots and pumps present. Though the field of synthetic self-powered transport is still in its infancy, it offers considerable promise as targeted delivery vehicles.[71–73] In efforts to design microdevices for *in vivo* biomedical applications, magnetically controlled microbots that can be injected into the body to perform diverse tasks like drug delivery and surgery have been developed.[74–76] In another report, chemically powered nanomachines have been modeled that utilize glucose as fuel to navigate through the bloodstream.[77] Ishiyama and co-workers have also fabricated micron-size magnetically driven spinning screws for potential applications in targeted drug delivery or to implant into tumor cells and destroy them thermally.[78]

Since the inception of synthetic nanomachines, we have made significant progress towards developing these nano/microtransporters into proof-of-concept tools for biomedical applications. One important application area is the design of autonomous microscale systems that convert chemical sensing into microfluidic pumping without using electronics, batteries, or other traditional means of translating a chemical detection event into a mechanical function. In these systems, the pump turns "on" only when a specific chemical signal is present.[70] Such nano/microscale pumps, with no moving parts, will provide precise control over the flow rate without the aid of an external power source and will provide the foundation for the next generation of smart meso- to molecular-scale devices.

While there has been significant progress, several hurdles remain before practical *in vivo* applications become a reality. First, the nano/microtransporters must be derived from biocompatible materials with appropriate surface functionalization to promote cell viability. Second, and equally important, is to design self-powered nano/microbots and pumps that can use fuels that are biocompatible, especially fuel sources present in the body. Ideally, the nano/microtransporters will employ enzymes as catalysts and fuels (*e.g.*, glucose) present in living systems.[79] Third, the transporters need to be powerful enough to move against fluid flows,[80] such as blood flow. Furthermore, the energy transduction mechanism should operate in high ionic medium present in biological fluids. Finally, the most "futuristic" scenario involves the design of populations of synthetic nano- and micromotors and pumps that have the ability to organize themselves intelligently, based on signals from each other and from their environment, to perform complex tasks. Particularly attractive are designs that allow the coordinated movement of particles with different functionalities that are *not* attached to each other, making it easier to transport and deliver cargo to the designated area. The recent discovery of particle assemblies that exhibit chemotaxis and

predator–prey behavior is a step in this direction.[81–83] In conclusion, it is possible to imagine a day when intelligent machines navigate through the human body and perform challenging tasks.[84,85]

Acknowledgements

We gratefully acknowledge NSF (DMR-0820404 and CBET-1014673), and AFoSR (FA9550-10-1-0509) for supporting our current research.

References

1 J. Sudimack and R. J. Lee, *Adv. Drug Delivery Rev.*, 2000, **41**, 147–162.
2 P. Stenberg, C. A. S. Bergström, K. Luthman and P. Artursson, *Clin. Pharmacokinet.*, 2002, **41**, 877–899.
3 K. Uekama, F. Hirayama and T. Irie, *Chem. Rev.*, 1998, **98**, 2045–2076.
4 Y. Qiu and K. Park, *Adv. Drug Delivery Rev.*, 2001, **53**, 321–339.
5 Q. A. Pankhurst, J. Connolly, S. K. Jones and J. Dobson, *J. Phys. D: Appl. Phys.*, 2003, **36**, R167–R181.
6 D. Patra, A. Sanyal and V. M. Rotello, *Chem.–Asian J.*, 2010, **5**, 2442–2453.
7 K. Kataoka, A. Harada and Y. Nagasaki, *Adv. Drug Delivery Rev.*, 2001, **47**, 113–131.
8 V. Torchilin, *Nat. Rev. Drug Discovery*, 2005, **4**, 145–160.
9 M. Pilarek, P. Neubauer and U. Marx, *Sens. Actuators, B*, 2011, **156**, 517–526.
10 O. Drory and N. Nelson, *Physiology*, 2006, **21**, 317–325.
11 B. Alberts, *Cell*, 1998, **92**, 291–294.
12 K. Kinbara and T. Aida, *Chem. Rev.*, 2005, **105**, 1377–1400.
13 M. I. Borges-Walmsley and A. R. Walmsley, *Trends Microbiol.*, 2001, **9**, 71–79.
14 K. S. Mckeegan, M. I. Borges-Walmsley and A. R. Walmsley, *Trends Microbiol.*, 2003, **11**, 21–29.
15 S. Murakami, R. Nakashima, E. Yamashita and A. Yamaguchi, *Nature*, 2002, **419**, 587–593.
16 M. Putman, H. W. Veen and W. N. Konings, *Microbiol. Mol. Biol. Rev.*, 2002, **64**, 672–693.
17 H. Hess and V. Vogel, *Rev. Mol. Biotechnol.*, 2001, **82**, 67–85.
18 A. Goel and V. Vogel, *Nat. Nanotechnol.*, 2008, **3**, 465–475.
19 L. Limberis, J. J. Magda and R. J. Stewart, *Nano Lett.*, 2001, **1**, 277–280.
20 K. J. Bohm, R. Stracke, P. Muhlig and E. Unger, *Nanotechnology*, 2001, **12**, 238–244.
21 H. Noji, R. Yasuda, M. Yoshida and K. Kinosita, *Nature*, 1997, **386**, 299–302.
22 G. L. Martin, V. van den Heuvel and C. Dekker, *Science*, 2007, **317**, 333–336.
23 Y. Hiratsuka, M. Miyata, T. Tada and T. Q. P. Uyeda, *Proc. Natl. Acad. Sci. U. S. A.*, 2006, **103**, 13618–13623.
24 N. Darnton, L. Turner, K. Breuer and H. C. Berg, *Biophys. J.*, 2004, **86**, 1863–1870.
25 T. Mirkovic, N. S. Zacharia, G. D. Scholes and G. A. Ozin, *Small*, 2010, **6**, 159–167.
26 T. Mirkovic, N. S. Zacharia, G. D. Scholes and G. A. Ozin, *ACS Nano*, 2010, **4**, 1782–1789.
27 Y. Hong, D. Velegol, N. Chaturvedi and A. Sen, *Phys. Chem. Chem. Phys.*, 2010, **12**, 1423–1435.
28 S. J. Ebbens and J. R. Howse, *Soft Matter*, 2010, **6**, 726–738.
29 J. Wang, *ACS Nano*, 2009, **3**, 4–9.
30 W. F. Paxton, S. Sundararajan, T. E. Mallouk and A. Sen, *Angew. Chem., Int. Ed.*, 2006, **45**, 5420–5429.
31 S. Sengupta, M. E. Ibele and A. Sen, *Angew. Chem., Int. Ed.*, 2012, **51**, 8434–8445.
32 E. M. Purcell, *Am. J. Phys.*, 1977, **45**, 3–11.
33 J. L. Anderson, *Ann. N. Y. Acad. Sci.*, 1986, **469**, 166–177.
34 W. F. Paxton, K. C. Kistler, C. C. Olmeda, A. Sen, S. K. St. Angelo, Y. Cao, T. E. Mallouk, P. E. Lammert and V. H. Crespi, *J. Am. Chem. Soc.*, 2004, **126**, 13424–13431.
35 S. Fournier-Bidoz, A. C. Arsenault, I. Manners and G. A. Ozin, *Chem. Commun.*, 2005, 441–443.
36 W. F. Paxton, A. Sen and T. E. Mallouk, *Chem.–Eur. J.*, 2005, **11**, 6462–6470.
37 S. Sundararajan, P. E. Lammert, A. W. Zudans, V. H. Crespi and A. Sen, *Nano Lett.*, 2008, **8**, 1271–1276.
38 S. Sundararajan, S. Sengupta, M. E. Ibele and A. Sen, *Small*, 2010, **6**, 1479–1482.
39 D. Kagan, R. Laocharoensuk, M. Zimmerman, C. Clawson, S. Balasubramanian, D. Kang, D. Bishop, S. Sattayasamitsathit, L. Zhang and J. Wang, *Small*, 2010, **6**, 2741–2747.
40 J. Burdick, R. Laocharoensuk, P. M. Wheat, J. Posner and J. Wang, *J. Am. Chem. Soc.*, 2008, **130**, 8164–8165.
41 D. Kagan, P. Calvo-Marzal, S. Balasubramanian, S. Sattayasamitsathit, K. M. Manesh, G. U. Flechsig and J. Wang, *J. Am. Chem. Soc.*, 2009, **131**, 12082–12083.
42 J. Wu, S. Balasubramanian, D. Kagan, K. M. Manesh, S. Campuzano and J. Wang, *Nat. Commun.*, 2010, **1**, 1–6.
43 J. Wu, S. Campuzano, C. Halford, D. A. Haake and J. Wang, *Anal. Chem.*, 2010, **82**, 8830–8837.
44 L. Baraban, D. Makarov, R. Streubel, I. Mönch, D. Grimm, S. Sanchez and O. G. Schmidt, *ACS Nano*, 2012, **6**, 3383–3389.
45 Y. F. Mei, A. A. Solovev, S. Sanchez and O. G. Schmidt, *Chem. Soc. Rev.*, 2011, **40**, 2109.
46 S. Balasubramaniam, D. Kagan, C. J. Hu, S. Campuzano, M. J. Lobo-Castañon, N. Lim, D. Y. Kang, M. Zimmerman, L. Zhang and J. Wang, *Angew. Chem., Int. Ed.*, 2011, **50**, 4161–4164.
47 S. Sanchez, A. A. Solovev, S. Schulze and O. G. Schmidt, *Chem. Commun.*, 2011, **47**, 698–700.
48 A. A. Solovev, Y. Mei, E. B. Ureña, G. Huang and O. G. Schmidt, *Small*, 2009, **5**, 1688–1692.
49 W. Gao, S. Sattayasamitsathit, J. Orozco and J. Wang, *J. Am. Chem. Soc.*, 2011, **133**, 11862–11864.
50 A. A. Solovev, S. Sanchez, M. Pumera, Y. F. Mei and O. G. Schmidt, *Adv. Funct. Mater.*, 2010, **20**, 2430–2435.
51 S. Sanchez, A. A. Solovev, S. Schulze and O. G. Schmidt, *Chem. Commun.*, 2011, **47**, 698–700.
52 A. A. Solovev, W. Xi, D. H. Gracias, S. M. Harazim, C. Deneke, S. Sanchez and O. G. Schmidt, *ACS Nano*, 2012, **6**, 1751–1756.

53 D. Kagan, S. Campuzano, S. Balasubramanian, F. Kuralay, G. Flechsig and J. Wang, *Nano Lett.*, 2011, **11**, 2083–2087.
54 S. Campuzano, J. Orozco, D. Kagan, M. Guix, W. Gao, S. Sattayasamitsathit, J. C. Claussen, A. Merkoci and J. Wang, *Nano Lett.*, 2012, **12**, 396–401.
55 J. Orozco, S. Campuzano, D. Kagan, M. Zhou, W. Gao and J. Wang, *Anal. Chem.*, 2011, **83**, 7962–7969.
56 S. Balasubramanian, D. Kagan, C. M. Hu, S. Campuzano, M. J. Lobo-Castañon, N. Lim, D. Y. Kang, M. Zimmerman, L. Zhang and J. Wang, *Angew. Chem., Int. Ed.*, 2011, **50**, 4161–4164.
57 D. J. Laser and J. G. Santiago, *J. Micromech. Microeng.*, 2004, **14**, 35–64.
58 A. Nisar, N. Afzulpurkar, B. Mahaisavariya and A. Tuantranont, *Sens. Actuators, B*, 2008, **130**, 917–942.
59 A. Dash and G. Cudworth Ii, *J. Pharmacol. Toxicol. Methods*, 1998, **40**, 1–12.
60 S. C. Jakeway, A. J. de Mello and E. L. Russell, *Fresenius' J. Anal. Chem.*, 2000, **366**, 525–539.
61 B. van der Schoot, S. Jeanneret, A. van den Berg and F. A. de Rooij, *Sens. Actuators, B*, 1992, **6**, 57–60.
62 J. Khandurina, T. E. McKnight, S. C. Jacobson, L. C. Waters, R. S. Foote and J. M. Ramsey, *Anal. Chem.*, 2000, **72**, 2995–3000.
63 A. T. Woolley, D. Hadley, P. Landre, A. J. de Mello, R. A. Mathies and M. A. Northrup, *Anal. Chem.*, 1996, **68**, 4081–4086.
64 Z. Lian, K. Jae-Mo, J. Linan, M. Asheghi, K. E. Goodson, J. G. Santiago and T. W. Kenny, *J. Microelectromech. Syst.*, 2002, **11**, 12–19.
65 E. Stemme and G. A. Stemme, *Sens. Actuators, A*, 1993, **39**, 159–167.
66 T. R. Kline, W. F. Paxton, Y. Wang, D. Velegol, T. E. Mallouk and A. Sen, *J. Am. Chem. Soc.*, 2005, **127**, 17150–17151.
67 M. E. Ibele, Y. Wang, T. R. Kline, T. E. Mallouk and A. Sen, *J. Am. Chem. Soc.*, 2007, **129**, 7762–7763.
68 I. K. Jun and H. A. Hess, *Adv. Mater.*, 2010, **22**, 4823–4825.
69 Y. Hong, M. Diaz, U. M. Córdova-Figueroa and A. Sen, *Adv. Funct. Mater.*, 2010, **20**, 1568–1576.
70 H. Zhang, K. Yeung, J. S. Robbins, R. A. Pavlick, M. Wu, R. Liu, A. Sen and S. T. Phillips, *Angew. Chem., Int. Ed.*, 2012, **51**, 2400–2404.
71 R. A. Freitas, *Int. J. Surg.*, 2005, **3**, 243–246.
72 J. Wang and W. Gao, *ACS Nano*, 2012, **6**, 5745–5751.
73 J. Wang, *Lab Chip*, 2012, **12**, 1944–1950.
74 B. J. Nelson, I. K. Kaliakatsos and J. J. Abbott, *Annu. Rev. Biomed. Eng.*, 2010, **12**, 55–85.
75 S. Tottori, L. Zhang, F. Qiu, K. K. Krawczyk, A. Franco-Obregón and B. J. Nelson, *Adv. Mater.*, 2012, **6**, 811–816.
76 W. Gao, D. Kagan, O. S. Pak, C. Clawson, S. Campuzano, E. Chuluun-Erdene, E. Shipton, E. E. Fullerton, L. Zhang, E. Lauga and J. Wang, *Small*, 2012, **8**, 460–467.
77 T. Hogg and R. A. Freitas, *Nanomedicine*, 2010, **6**, 298–317.
78 K. Ishiyama, M. Sendoh and K. I. Arai, *J. Magn. Magn. Mater.*, 2002, **242–245**, 41–46.
79 H. S. Muddana, S. Sengupta, T. E. Mallouk, A. Sen and P. J. Butler, *J. Am. Chem. Soc.*, 2010, **132**, 2110–2111.
80 S. Sanchez, A. A. Solovev, S. M. Harazim and O. G. Schmidt, *J. Am. Chem. Soc.*, 2011, **133**, 701–703.
81 M. I. Ibele, P. E. Lammert, V. H. Crespi and A. Sen, *ACS Nano*, 2010, **4**, 4845–4851.
82 M. Ibele, T. E. Mallouk and A. Sen, *Angew. Chem., Int. Ed.*, 2006, **48**, 3308–3312.
83 G. von Maltzahn, J. Park, K. Y. Lin, N. Singh, C. Schwöppe, R. Mesters, W. E. Berdel, E. Ruoslahti, M. J. Sailor and S. N. Bhatia, *Nat. Mater.*, 2011, **10**, 545–552.
84 S. David, *Fantastic Voyage Producer*, Twentieth Century Fox Film Corporation, 1966.
85 M. Crichton, *Prey*, Harper Collins, New York, 2002.